

# Effect of KCl on the characteristics of PvdF-Co-Hfp-based nanocomposite polymer electrolytes

N Ramaiah<sup>1,3\*</sup> , V Raja<sup>2</sup> and C Ramu<sup>1</sup>

<sup>1</sup>Department of Physics, Vikrama Simhapuri University Postgraduate Center, Kavali 524201, A.P, India

<sup>2</sup>Department of Physics, SVSSC Government Degree College, Sullurpet 524121, A.P, India

<sup>3</sup>Department of Physics, SVREC, Nandyal 518501, A.P, India

Received: 07 January 2023 / Accepted: 03 July 2023 / Published online: 6 August 2023

**Abstract:** The synthesised films have been characterised via different techniques. Structural studies were carried out using the XRD technique. TGA/DSC analysis revealed that the micro-porous polymer membrane is thermally stable up to 450 C. The electrical measurement for all samples have been carried out in frequency range 42 Hz–5 MHz and temperature range of 30–110 C by Impedance Spectroscopy. The FTIR study showed many excellent spectral changes. These spectral changes indicate an increase in crystallinity, strong molecular bonds, and some crystal phase transitions. The large values of dielectric constant in the low frequency region of the particular polymer electrolyte specimen containing 15% wt% alkali metal may be due to an enhanced level of charge carrier storage at the electrolyte–electrode interface, resulting in an increase in capacitance. The temperature dependent ac ionic conductivity shows the highest ionic conductivity of  $1.35 \times 10^{-4} \text{ Scm}^{-1}$  was found at 333 K for the concentration of 85 Wt% PVdF-CO-HFP: 15 Wt% KCl: 5 Wt% TiO<sub>2</sub> of the polymer electrolytes with an activation energy value of 0. As a result, alkali metal can significantly improve the structural, conductivity and dielectric properties of nanocomposite polymer electrolytes over ordinary polymer electrolytes, providing a new method for preparing composites with high structural and dielectric properties.

**Keywords:** PVDF-co-HFP; Dielectrical properties; XRD; TiO<sub>2</sub> nanoparticles; TGA; Impedance analysis

## 1. Introduction

Recent developments in solid state polymer batteries, electrochemical sensors, and electrochromic devices have stoked interest in solid state ionics due to their potential utility in these fields [1–3]. These solid-state batteries offer a number of benefits, including increased energy density, solvent-free operation, leak resistance, ease of processing, and light weight. Electrolytes are the most significant and active components of solid-state batteries, and they make up the majority of them [4, 5]. Many investigations on these polymer electrolytes have been conducted in order to better understand the principles driving their structure, capacity to solvate ions, and high dielectrical characteristics [6, 7]. Solid state batteries based on poly(vinylidene fluoride) (PVDF), poly(vinyl pyrrolidone) (PVP), poly(-vinyl alcohol) (PVA), and poly(vinyl alcohol) (PVA) have

been studied in an attempt to study the possibility of fabricating Solid state batteries based on polymers other than widely studied polymers such as poly(ethylene oxide) (PEO) and poly(propylene oxide) (PPO) [8, 9].

In this process of preparing polymer electrolytes from compositions of alkali metal salts has numerous practical applications based on their superior attributes. Because of that, coordinated complexes of alkali metals (AM) in polymer hosts are widely used. Interactions between alkali metal ions and polymers have been shown to have a significant influence on the behaviour of the polymers and their new properties. A few attempts have been made to use polymer electrolytes based on potassium ion complexed films [10, 11]. The main advantage of using potassium metal ions is their availability in abundance at a cheaper cost than lithium. Furthermore, more softness in the material makes it easier to achieve good contact with other components in the battery. Still, no attention is paid to potassium salt complexed PVDF-co-HFP/TiO<sub>2</sub>-based polymer electrolytes [12].

\*Corresponding author, E-mail: ramn231983@gmail.com

These alkali metal polymer electrolytes play a very essential role as the primary medium for ionic conduction in the SSBs and can be in the form of a liquid, gel, or solid. Among these types of polymer electrolyte systems, nanocomposite polymer electrolytes [NCPEs] have many advantages, such as high ionic conductivity, high energy density, leakproof, solvent-free conditions, wide electrochemical stability windows, easy processability, and lightweight [13, 14]. To further improve the ionic conductivity of GPEs, inorganic fillers in the form of nanoparticles, such as  $\text{SiO}_2$ ,  $\text{ZnO}$ ,  $\text{TiO}_2$ ,  $\text{Al}_2\text{O}_3$ , and molecular sieves, have been introduced into the polymer matrix. Despite this, high ionic conductivity even though most SPEs exhibit poor wetting ability and restricted ionic conductivities; they can be obtained only when a very small amount of filler is added. In contrast, the better hardness of GPEs can normally be obtained with a higher inorganic filler content [15]. This indicates, therefore, it is important to find the optimum content of inorganic filler.

The mechanism of ion conduction in nanocomposite polymer electrolytes [NCPEs] is currently unknown. As a result, it is crucial to understand the ion transport and polymer segmental relaxation mechanisms in polymer electrolytes [16, 17]. Dielectric relaxation events can be used to better understand ion transport behaviour and obtain information on ionic and molecular interactions in polymer electrolytes. Ion transit is influenced by the degree of salt dissociation and its concentration, the dielectric constant of the host polymer, the degree of ion aggregation, and the mobility of polymer chains [18, 19]. Dielectric relaxation and frequency dependent conductivity are affected by the mobility of charged species and dipoles in the polymer. According to a survey of the literature, few studies on potassium ion complexed PVDF-co-Hfp/ $\text{TiO}_2$  electrolyte systems have been conducted. Given the aforementioned, the goal of this research is to conduct dielectric and electrical conductivity tests on a polymer electrolyte system containing a PVDF-co-HFP/ $\text{TiO}_2$ /AM complex [20].

## 2. Experimental details

### 2.1. Materials

The host polymer, PVDF-co-HFP (Mw 400,000, Sigma-Aldrich), as well as the ionic dopant, KCl(AM) (Mw 363.53 g mol<sup>-1</sup>, Sigma-Aldrich), nanofiller  $\text{TiO}_2$  (> 100 nm, Sigma-Aldrich), and tetrahydrofuran (THF) solvent from Merck Milliopore, Germany These materials were dried and used to make nanocomposite polymer electrolytes (NCPEs). None of the materials described

above were modified or treated in any way before being employed.

### 2.2. Preparation of nanopolymer electrolyte membranes

PVdF-co-HFP + KCl +  $\text{TiO}_2$ -based nanocomposite polymer electrolyte films (NCPEs) were created using a simple solvent casting approach. The PVDF-co-HFP:  $\text{TiO}_2$  ratio was kept constant at 80: 5 during the preparation of specimens. THF was used as the common solvent to maintain the homogeneous solution of 80 PVDF-co-HFP: 5  $\text{TiO}_2$  complexes, into which sufficient amounts of KCl salts were also disseminated. To eliminate any remnants of THF, the solution combination was cast onto clean glass petri dishes and dried in a vacuum oven at 50 °C for 12 h. After the complete elimination of THF, all specimens belonging to the polymer electrolyte system, 80 wt per cent PVDF-co-HFP: 5 wt per cent  $\text{TiO}_2$ , + x wt per cent KCl (where  $x = 0, 5, 10, \text{ and } 15$ , respectively) were generated. This process produced mechanically stable, freestanding, and flexible films, which were then stored in a vacuum desiccator for 24 h before being studied in detail.

### 2.3. Characterisation techniques

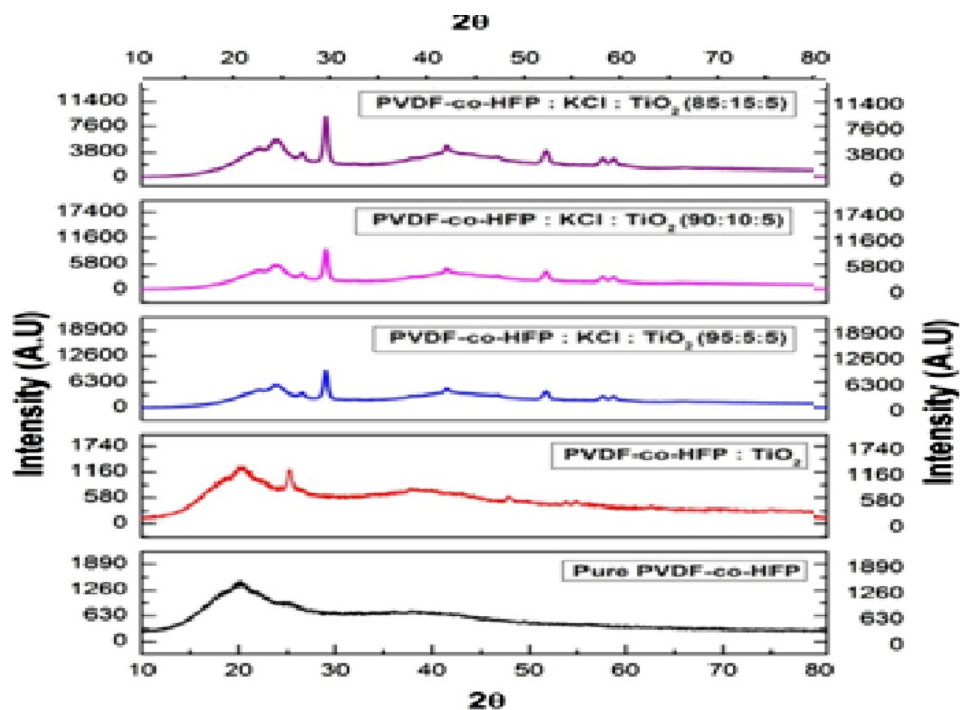
X-ray diffraction pattern of the samples was obtained using SHIMADZU-XRD-6000 diffractometer with Cu-K $\alpha$  radiation (wavelength = 0.1541 nm) as the source at 40 kV and a scanning range between 10° and 80°. FTIR spectroscopy studies were performed using a 400–4000 cm<sup>-1</sup> BRUKER-FTIR-ATR spectrometer with a 4 cm<sup>-1</sup> spectral resolution. Thermogravimetric and differential thermal analysis (TG–DTA) studies were performed with the aid of a NETSZCH thermogravimetric analyzer at a scan rate of 283 K/min in the temperature range of room temperature to 873 K. The AC impedance studies were carried out for the as prepared NCPE films with stainless steel as the blocking electrodes, using a computer-controlled electrochemical analyzer (Model: CHI-600E, Make: CH-instrument) in the frequency range of 40 Hz–1 MHz at room temperature to 353 K.

## 3. Results and discussion

### 3.1. X-ray diffraction analysis

Figure 1 shows the X-ray diffraction patterns of pure PVDF-co-HFP, KCl, and  $\text{TiO}_2$  nanofiller doped NCPEs at various concentrations. The XRD pattern of PVDF-co-HFP clearly shows a peak around 21.69°, as seen in Fig. 1. The strength of the peak lowers when  $\text{TiO}_2$  nanofiller and an

**Fig. 1** X-ray diffraction patterns of pure PVDF-co-HFP, KCl, and TiO<sub>2</sub> nanofiller doped NCPFs at various concentrations



alkali metal electrolyte like KCl are introduced to the PVDF-co-HFP polymer. The crystalline peaks of TiO<sub>2</sub> contained in the NCPFs were clearly indicated in Fig. 1, which shows the tetragonal structure of TiO<sub>2</sub> nanoparticles. The miller indices (021), (200), (220), (102), (211), (110) and (311) were determined from XRD data of TiO<sub>2</sub> nanoparticles at 25.6°, 38.2°, 49.3°, 53°, 54.0°, 55.6°, and 62.925°, respectively. The crystalline character of the produced TiO<sub>2</sub>NPs contained in the inner NCPFs was clearly expressed in Fig. 1; this result implies that when the concentration of KCl rises, the amorphous character of the NCPFs increases. The rise in amorphous nature is due to a strong interaction between the polymer and the K<sup>+</sup> ions, which causes the intermolecular connection between the polymer chains to decrease. As a result, the degree of crystallinity decreases, implying an increase in the amorphous zone. The energy barrier to the segmental motion of the PVDF-co-HFP NCPFs is reduced as the amorphous form of the NCPFs increases. This amorphous form leads to increased ionic conductivity and ion transport, as evidenced by the current work's conductivity measurements.

### 3.2. TG-DTA analysis

TG-DTA thermograms of KCl and TiO<sub>2</sub> nanofiller doped PVDF-co-HFP NCPFs are shown in Fig. 2. As shown in Fig. 2, all prepared samples go through two separate weight loss stages. The initial weight loss of all prepared samples happened at temperatures ranging from 35 °C to 149 °C. This region had a weight loss of 11–13%, which

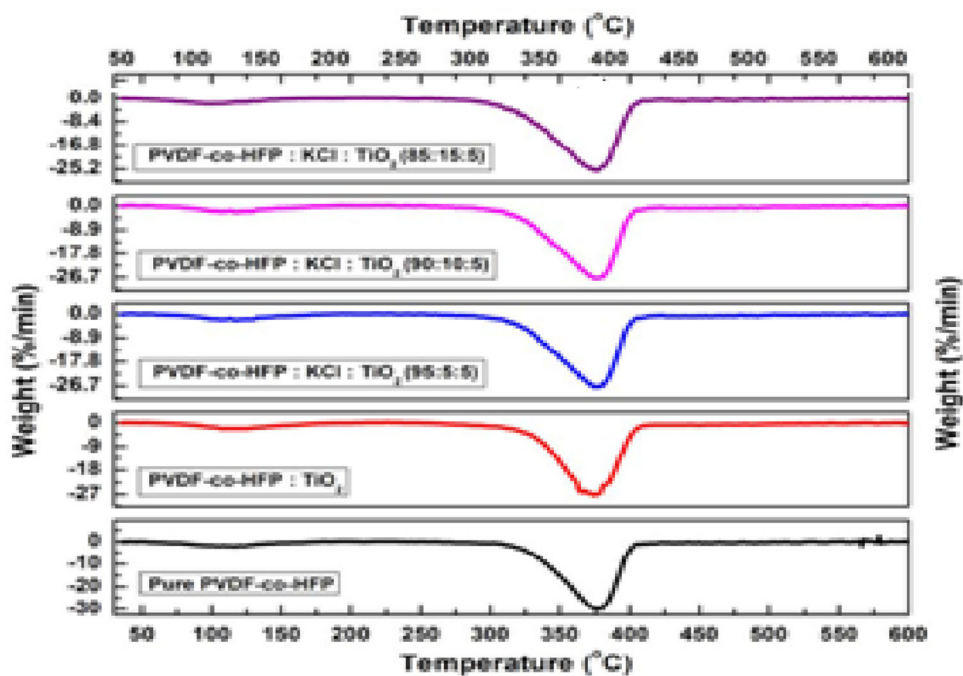
was attributable to the evaporation of moisture received by the sample during sample loading. The deterioration of samples over 250 °C in a multi-step process (Fig. 2) implies that the current samples are mixed polymers. The temperature range 281 °C–349 °C resulted in the greatest weight loss of the prepared samples, with a loss of 63–67%. The presence of a chemical degradation process resulting from bond scission (carbon–carbon bonds) in the polymeric backbone is revealed by the significant weight loss in the second decomposition stage.

Pure PVDF-co-HFP film decomposes at a temperature of 419 °C. *T<sub>d</sub>* values for KCl, TiO<sub>2</sub> doped films were lower than those for pure films. There are two stages of weight reduction, each with their own peak temperatures and weight loss percentages (Table 1). A higher KCl content in a polymer, results in lower melting and breakdown temperatures. As a result, 15 wt% of KCl, TiO<sub>2</sub> doped NCPFs have a more amorphous nature than 5 and 10 wt% NCPFs.

### 3.3. FTIR analysis

Figure 3 shows the FTIR spectra of TiO<sub>2</sub> nanofiller and KCl-doped PVDF-co-HFP NCPFs with varied concentrations. FTIR results state that the main absorption band noticed at in the range of 3517 cm<sup>-1</sup>–3436 cm<sup>-1</sup> is due to the –OH functional group present in the pure PVDF-co-HFP and doped NCPFs. The another peaks observed in the range of 2933 cm<sup>-1</sup>–2911 cm<sup>-1</sup>, 1625 cm<sup>-1</sup>–1603 cm<sup>-1</sup> and 1384 cm<sup>-1</sup>–1357 cm<sup>-1</sup> is owing to the C–H stretching, C–O stretching and C–H bending vibrations of CH<sub>2</sub>,

**Fig. 2** TG-DTA spectral curves for pure PVDF-co-HFP and of TiO<sub>2</sub>, KCl doped PVDF-co-HFP NCPFs



respectively. The remaining peaks noted at  $1193\text{ cm}^{-1}$ – $1146\text{ cm}^{-1}$  and  $842\text{ cm}^{-1}$ – $826\text{ cm}^{-1}$  is owing to the C–C stretching vibrations and C–X (F, Cl) stretching vibrations, respectively. For 5wt% and 15wt% KCl doped films, the strength of this band is decreasing, and it is completely gone for 15wt% KCl doped films. This could be due to ionic association caused by charge redistribution during the creation of ionic pairs and aggregations (Table 2).

#### 3.4. Impedance analysis of KCl and TiO<sub>2</sub> nanofiller doped PVDF-co-HFP NCPFs

For pure PVDF-co-HFP and KCl and TiO<sub>2</sub> doped polymer NCPFs, the typical real ( $Z'$ ) and imaginary ( $Z''$ ) sections of the impedance data displayed in the complex impedance plane are shown in Fig. 4. These two separate zones can be seen in the figure. A low-frequency inclined spike and a high-frequency semicircular arc. As a result, a given sample frequency response may be represented by an equivalent circuit made up of a parallel combination of the circuit elements  $R$  (resistance) and  $C$  (capacitance). The bulk electrical resistance ( $R_b$ ) of the material is obtained from these Cole–Cole plots by plotting the intercept of the low-frequency side on the X-axis. The intercept of the semicircle (bulk resistance) on the real axis tends to decrease with increasing temperature and salt concentration, according to the Cole–Cole plots of several electrolyte films with changing salt concentrations at various temperatures. As temperature rises, ionic mobility and the amount

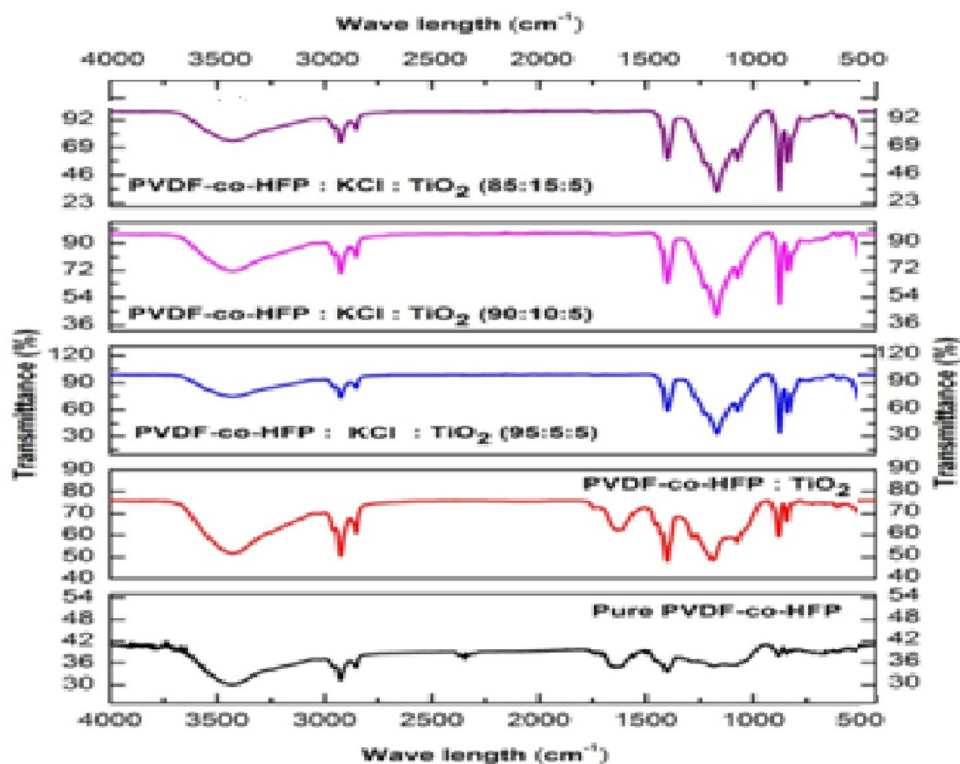
of carrier ions increase, which results in a reduction in the polymer electrolyte's resistance. The free volume of the polymer matrix, which can be represented by a resistor, may be used for ion migration. The stationary polymer chains polarise in the alternating field, which can be modelled as a capacitor. The semicircle at high frequency can be visible in all samples because ionic migration and bulk polarisation are physically parallel. It was discovered that conductivity increased as salt concentrations increased. The conductivity values of several complexes at room temperature are summarised in Table 3. PVDF-co-HFP NCPF conductivities and activation energies at various compositions.

#### 3.5. Temperature dependence conductivity of PVDF-co-HFP NCPFs

The  $\log\sigma$  vs.  $1000/T$  graphic represents the ionic conductivity of a polymer as a function of temperature. The fluctuation of  $\log\sigma$  with inverse absolute temperature for various PVDF-co-HFP NCPFs of different compositions is shown in Fig. 5. According to these results, the ionic conductivity of the complexed systems does not display an abrupt increase with temperature, indicating that these electrolytes have a totally amorphous structure. The figures show that when the temperature rises, the ionic conductivity of all the complexes increases, which is consistent with the idea of Armand et al.

**Table 1** TG-DTA curves data for pure PVDF-co-HFP and of NaCl, TiO<sub>2</sub> doped PVDF-co-HFP NCPFs

Polymer Composition (Wt%)	Temperature (°C)			Weight loss (Wt%)	
	Start	End	Peak (T <sub>p</sub> )	Partial	Total
Pure PVDF-co-HFP	58	175	116	16	92
	320	419	369	76	
PVDF-co-HFP:TiO <sub>2</sub> (95:5)	47	161	104	15	86
	298	403	351	71	
PVDF-co-HFP:TiO <sub>2</sub> :KCl (95:5:5)	40	149	94	13	80
	299	401	349	67	
PVDF-co-HFP:TiO <sub>2</sub> :KCl (90:5:10)	36	143	89	12	78
	286	394	340	66	
PVDF-co-HFP:TiO <sub>2</sub> :KCl (85:5:15)	35	140	87	11	74
	281	379	329	63	

**Fig. 3** FTIR spectra of pure PVDF-co-HFP film and TiO<sub>2</sub> and KCl doped PVDF-co-HFP NCPFs with different ratios

The activation energy is a mixture of charge carrier creation energy and ion migration energy. As a result, the value of  $E$  may be due to the energy required to create a conductive environment for ion migration. Table 3 shows the conductivity and activation energy values of the polymer electrolytes.

The activation energy decreases with increasing salt concentration, due to a lower energy barrier to the segmental motion of the polymer matrix, as shown in the table.

It is worth noting that for practical applications, a polymer electrolyte with low activation energy is preferable.

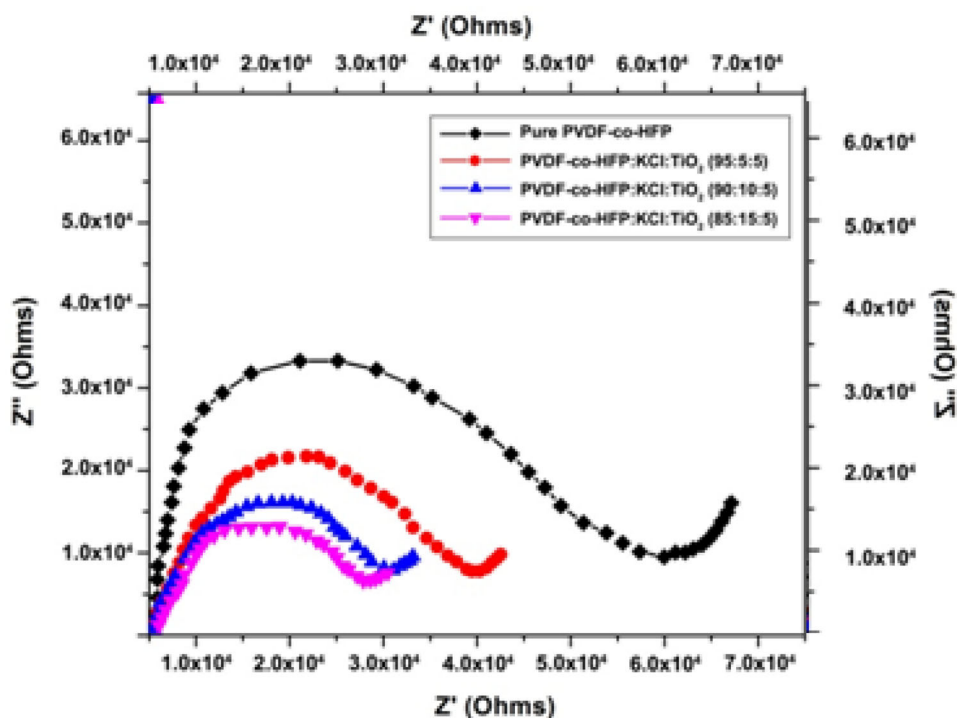
### 3.6. Frequency dependence of total conductivity

Figure 6 illustrates the frequency dependence of conductivity in pure PVDF-co-HFP, KCl and nano TiO<sub>2</sub> NCPFs at room temperature. Two distinct tendencies emerged in each of these conductivity spectra a frequency-independent conductivity at low frequency as a plateau zone and a



**Table 2** Absorption band assignments for pure PVDF-co-HFP and of TiO<sub>2</sub> and KCl doped PVDF-co-HFP NCPFs

Various absorption bands (cm <sup>-1</sup> )	Pure PVDF-co-HFP (cm <sup>-1</sup> )	PVDF-co-HFP:TiO <sub>2</sub> : KCl (95:05:5)	PVDF-co-HFP:TiO <sub>2</sub> : KCl (90:5:10)	PVDF-co-HFP:TiO <sub>2</sub> : KCl (85:5:15)
-OH stretching	3436	3497	3511	3517
C-H stretching (CH <sub>2</sub> )	2931	2928	2919	2911
C-O stretching (C = O)	1624	1611	1608	1603
C-H Bending (CH <sub>2</sub> )	1474	1369	1363	1357
C-C stretching	1196	1167	1156	1146
C-X (F,Cl)stretching	881	833	829	827

**Fig. 4** Cole–Cole plots of KCl and TiO<sub>2</sub> doped PVDF-co-HFP NCPFs**Table 3** Conductivities and activation energies of PVDF-co-HFP NCPFs at different compositions

S.No	Sample	Conductivity (Scm <sup>-1</sup> )	Activation energy E (eV)
1	Pure PVDF-co-HFP	$1.7 \times 10^{-7}$	0.43
2	PVDF-co-HFP:KCl:TiO <sub>2</sub> (95:05:5)	$2.9 \times 10^{-4}$	0.32
3	PVDF-co-HFP:KCl:TiO <sub>2</sub> (90:10:5)	$2.1 \times 10^{-4}$	0.29
4	PVDF-co-HFP:KCl:TiO <sub>2</sub> (85:15:5)	$1.35 \times 10^{-4}$	0.22

frequency-dependent conductivity at high frequency as a dispersion region, as shown in the figure. The conductivity increases as the frequency rises in the high frequency domain. On the other hand, high frequency conductivity

appears to be less temperature-dependent than low-frequency conductivity.

$$\sigma(\omega) = A\omega^n$$

where  $\sigma_{ac}(\omega)$  is the ac conductivity at high frequencies, which is frequency-dependent conductivity. A is a

**Fig. 5** Arrhenius fit of  $\log \sigma_{ac}$  versus  $1000/T$  of pure PVDF-co-HFP, KCl and  $TiO_2$  doped NCPFs

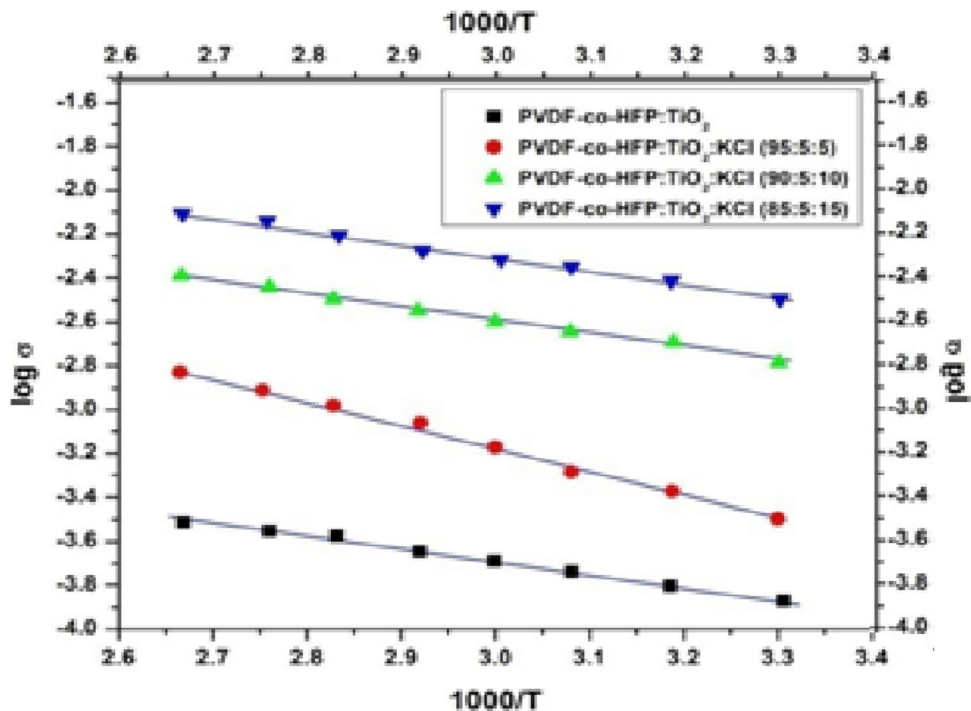


**Fig. 6**  $\log \sigma_{ac}$  versus  $\log \omega$  plots of pure PVDF-co-HFP, KCl and  $TiO_2$  doped NCPFs

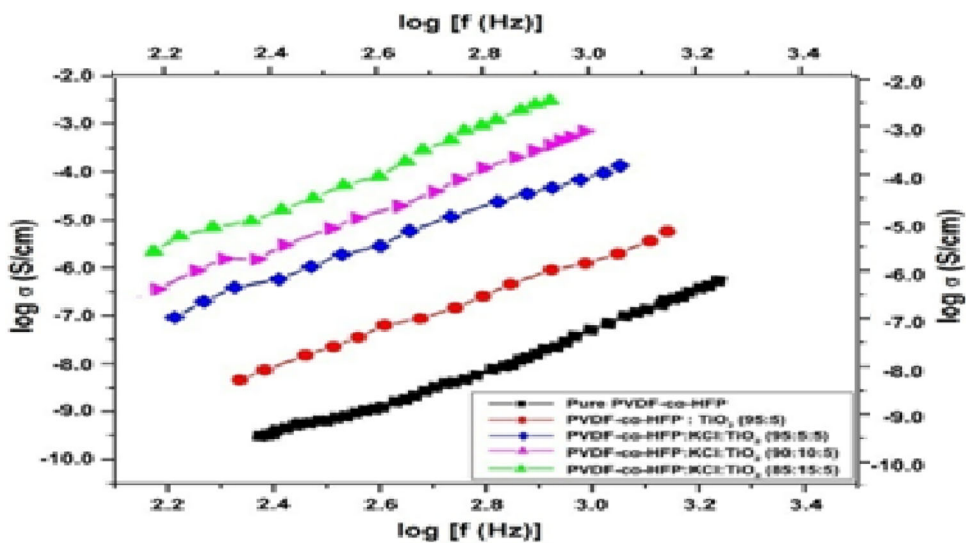
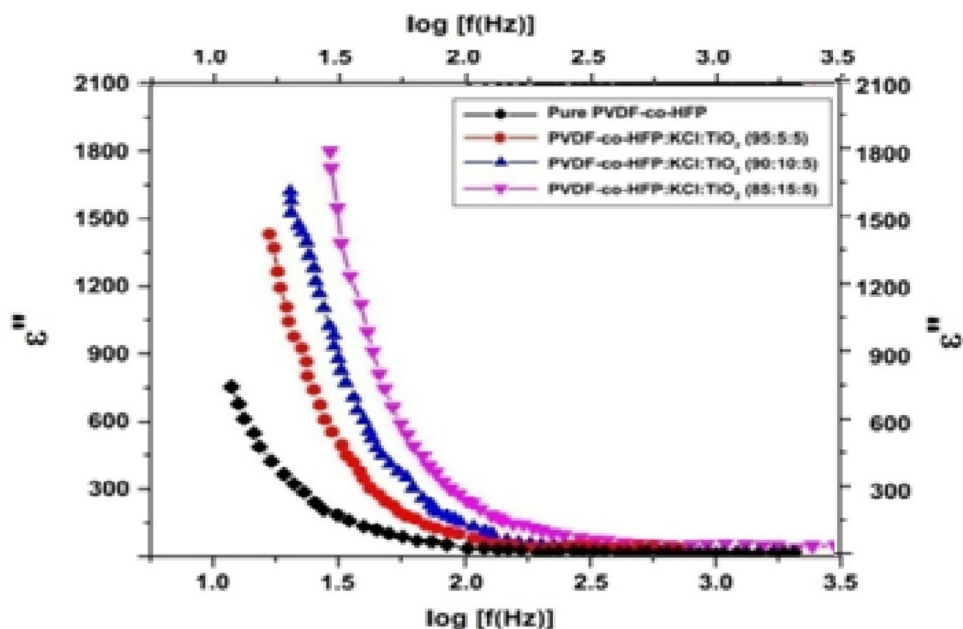


**Table 4** PVDF-co-HFP NCPFs conductivity and frequency exponent n

S.No	Sample	Conductivity ( $S\text{cm}^{-1}$ )	n
1	Pure PVDF-co-HFP	$1.7 \times 10^{-7}$	0.96
2	PVDF-co-HFP: $TiO_2$ (95:05)	$1.1 \times 10^{-6}$	0.68
3	PVDF-co-HFP:KCl: $TiO_2$ (95:05:5)	$2.9 \times 10^{-4}$	0.62
4	PVDF-co-HFP:KCl: $TiO_2$ (90:10:5)	$2.1 \times 10^{-4}$	0.59
5	PVDF-co-HFP:KCl: $TiO_2$ (85:15:5)	$1.35 \times 10^{-4}$	0.52

**Fig. 7** Dielectric permittivity vs.  $\log \omega$  plots of pure PVDF-co-HFP, KCl and  $\text{TiO}_2$  doped NCPFs



temperature-dependent and frequency-independent parameter,  $\omega = 2\pi f$  is the angular frequency, and  $n$  is the temperature-dependent frequency exponent that ranges from 0 to 1. This power-law behaviour is a universal property of materials related to the dynamics of hopping conduction which has been widely observed in disordered materials such as ionically conducting glasses, conducting polymers and doped crystalline solids. It is generally thought to be reflected in the mechanism of charge transport behaviour of charge carriers.

The equation ( $\sigma(\omega) = \sigma_{dc} + \sigma_{ac}$ ) was used to fit the conductivity spectra of polymer electrolytes. The parameter  $n$  was calculated using the slopes of the high-frequency dispersion lines. Table 4 shows the values of  $n$  for several complexed polymer electrolytes at room temperature as a function of salt concentration. According to the table, the  $n$  value is between 0 and 1 and declines as the salt concentration rises, which could be related to the development of free sites for ion transport.

### 3.7. Dielectric studies of PVDF-co-HFP NCPFs

#### 3.7.1. Frequency dependence of dielectric permittivity ( $\epsilon'$ )

At room temperature, the dielectric permittivity ( $\epsilon'$ ) of pure PVDF-co-HFP polymer, KCl and  $\text{TiO}_2$  doped PVDF-co-HFP NCPFs varies with frequency, as shown in Fig. 7

The graphs show that the dielectric permittivity declined monotonically with increasing frequency, reaching a constant value at higher frequencies, the contribution of charge accumulation at the electrode–electrolyte interface is due to the low-frequency dispersion area. This confirms the

non-Debye type behaviour by indicating that wide spread electrode polarisation and space charge effects are wide spread. The dielectric constant is proportional to  $\omega^{-(1-n)}$  for low frequencies, where  $n$  is in the range of 0.1–0.2.

The periodic reversal of the electric field occurs so quickly at higher frequencies that there is no extra ion diffusion in the field's direction. As a result,  $\epsilon'$  decreases with increased frequency in all nanopolymer electrolyte samples. As a result, the dielectric constant is almost frequency independent at higher frequencies because periodic reversals of the field occur so quickly at high frequencies that charge carriers are unable to orient themselves in the field direction, resulting in the observed decrease in the dielectric constant. The general dependence  $\omega^{-(1-k)}$ , with  $k$  in the range 0.8–0.9 for common ionic conductor materials, yields the high-frequency non-Debye region.

## 4. Conclusion

The PVDF-co-HFP: KCl:  $\text{TiO}_2$  nanocomposite polymer electrolytes have been fabricated using the solution casting technique. The nanocomposite polymer electrolyte film is flexible and offers relatively high ionic conductivity at room temperature. The XRD and FTIR confirm the complex formation. The thermal stability of the film was confirmed by TG–DTA studies. AC impedance analysis is confirming the conductivity of polymer electrolytes. The magnitude of ionic conductivity increased with the increase in salt concentration and temperature. PVDF-co-HFP:  $\text{TiO}_2$  (85:5) complexed with 15 wt% KCl salt showed the highest ionic conductivity ( $1.35 \times 10^{-4} \text{ S cm}^{-1}$ ) and low



activation energy (0.22 eV). The complex impedance plots (Cole–Cole plots) indicate that PVDF-co-HFP: TiO<sub>2</sub> blends can be effectively doped with KCl to enhance their conductivity. From the dielectric analysis, the dielectric constant rises owing to the departure of ions and the vibration of the polymer chain sector, thus increasing the conductivity. These results suggest the application of nanocomposite electrolyte films in developing solid-state flexible electrochemical devices.

#### Declarations

**Conflict of interest** All the authors declare that they have no conflict of interest.

#### References

- [1] R A Huggins *Solid State Ionics* **134** 179 (2000)
- [2] R Dhilip Kumar, S Nagarani and V Sethuraman *Chemical Papers* **76** 3371 (2022)
- [3] T Onuma et al *ACS Omega* **3** 159 (2018)
- [4] M Shao et al *Chinese Chemical Letters* **34** 107767 (2022)
- [5] G Rollo-Walker *Polymers (Basel)* **13** 4127 (2021)
- [6] M Gnana kiran et al *International Journal of Ambient Energy* (2022)
- [7] Z Xiao et al *Journal of Membrane Science* **576** 182 (2019)
- [8] M Sadiq et al *ACS Omega* **7** 40116 (2022)
- [9] N Satyanarayana *Ionics* **19** 1835 (2013)
- [10] W Wang and P Alexandridis *Polymers* **8** 387 (2016)
- [11] R Kumar, S Sahoo, E Joanni et al *Nano Research* **12** 2655 (2019)
- [12] K-Y Zhang et al *Materials Today* **54** 189 (2022)
- [13] Z Long, J Miyake and K Miyatake *Sulfonated Bull Chem. Soc. Jpn.* **93** 338 (2020)
- [14] S Hegde, V Ravindrachary, S D Praveena, B Guruswamy and R N Sagar *Ionics* **26** 2379 (2020)
- [15] M A M Saeed and O G Abdullah *Membranes* **10** 262 (2020)
- [16] N Kumar, M Sahu and D K Sahu *J Solid State Electrochem* **26** 1613 (2022)
- [17] S Seghaier, N Kamoun, R Brini and A B Amara *Mater Chem Phys* **97** 71 (2006)
- [18] S Mondal and D Basak *Surfaces Interfaces* **31** 102090 (2022)
- [19] I S Elashmawi and N H Elsayed *Polym Bull* **77** 949 (2020)
- [20] A Das et al *In Polymer Electrolytes for Energy Storage Devices* **133** (2021)

**Publisher's Note** Springer Nature remains neutral with regard to jurisdictional claims in published maps and institutional affiliations.

Springer Nature or its licensor (e.g. a society or other partner) holds exclusive rights to this article under a publishing agreement with the author(s) or other rightsholder(s); author self-archiving of the accepted manuscript version of this article is solely governed by the terms of such publishing agreement and applicable law.